A SLOWLY MOVING PLASMOID ASSOCIATED WITH A FILAMENT ERUPTION

N. GOPALSWAMY and M. R. KUNDU

Astronomy Program, University of Maryland, College Park, MD 20742, U.S.A.

(Received 6 June, 1988; in final form 18 November, 1988)

Abstract. We report the imaging observations of a slowly moving type IV burst associated with a filament eruption. This event was preceded by weak type III burst activity and was accompanied by a quasi-stationary continuum that persisted for several hours. The starting times and speeds of moving type IV burst and the erupting filament are nearly the same, implying a close physical relation between the two. The moving type IV burst is interpreted as gyrosynchrotron emission from a plasmoid containing a magnetic field of ~ 1–2 G and nonthermal electrons of density $\sim 10^5$–10^6 cm^{-3} with a relatively low average energy of ~ 50 keV.

1. Introduction

An understanding of the association of moving type IV bursts (or the coronal mass ejections in general) with other near-surface solar phenomena will be useful in identifying the origin of the ejections. Nearly three decades of observation of moving type IV bursts has shown that many of them are associated with flares, or more frequently with some form of filament activity (see, e.g., Robinson, 1978). Even during flares, filament eruptions occur frequently (Smith and Ramsey, 1964; Martin and Ramsey, 1972) and it is known that these types of flares are more commonly associated with coronal mass ejections (Munro *et al.*, 1979). Therefore, the ejection of chromospheric material (whether flare associated or not) seems to be an important near-surface indication of mass ejections. Although cool prominence material is found in the cores of several mass ejections, heating of the prominence material to coronal temperatures has also been observed (Webb and Jackson, 1981). Moving type IV bursts may be associated with this type of heated prominence material (e.g., Stewart *et al.*, 1974). First conclusive evidence of hot, dense, white light material being associated temporally and spatially with a moving type IV source has been provided by Stewart *et al.* (1982). Therefore, we expect the eruption and heating of the prominence material to be linked to the nonthermal particles in the moving type IV plasmoid. In fact, recent numerical models show that the dynamic disappearance of filaments induces currents in the neutral sheet below, which might lead to flaring (Kuin and Martens, 1986). As seen in Hα, the filament eruption begins slowly at or before the onset phase of a flare, and becomes explosive during the impulsive phase of the flare (Tandberg-Hanssen, Martin, and Hansen, 1980; Moore, Horwitz, and Green, 1984). This could be taken to suggest that small-scale reconnections may take place below the filament before the explosive lift-off of the filament. Several examples which show concretely that prominences may disappear, by the slow or rapid flow of material or by the violent eruptives, have been provided in the

Solar Physics **122** (1989) 91–110.

literature (e.g., Smith and Ramsey, 1964; Martin and Ramsey, 1972; Martin, 1973).

Slowly moving type IV bursts and coronal mass ejections have become important topics of current interest from another point of view: generation of slow mode shocks and nonthermal particles (Hundhausen, Holzer, and Low, 1987; Kundu, 1987). A slowly moving type IV burst cospatial with a white light CME, classified as a coronal streamer disruption event (Illing and Hundhausen, 1986), was reported by Kundu (1987). The moving type IV burst of 1986, February 2 was also slowly moving and occurred during a filament disappearance in the presence of streamers undergoing changes typical of streamer disruption events in white light. Three types of radio emissions were observed: moving type IV bursts, quasi-stationary continuum and weak type III bursts. A preliminary investigation using Clark Lake observations along with *Solar Geophysical Data* and *Nobeyama Radiospectrograph Data* show that this continuum persisted for several days (Gopalswamy and Kundu, 1988a).

The Clark Lake multifrequency radioheliograph can observe both the quiet Sun and weak bursts simultaneously. The imaging observations can be used to compare radio sources with features from observations at other wavelengths in order to establish the location of the bursts relative to the large-scale coronal structures such as streamers. Comparison of the locations of various types of radio bursts having a common activity center near the solar surface will reveal the structure of magnetic fields in the upper corona as most of the nonthermal particles are guided or trapped by these magnetic fields. In the present event, we compare the quiet sun features observed in radio with the Mauna Loa *K*-coronameter images to understand the dynamic nature of the corona in which the radio bursts occurred. In this paper, we use the relative timing of the moving type IV burst and the filament activity to understand the possible origin of the plasmoid and the nonthermal particles trapped within it that generate the observed radiation. We also discuss the two possible emission mechanisms, viz., the plasma and gyrosynchrotron emissions and derive some physical characteristics of the plasmoid. We also briefly discuss the implications of the positional and temporal relation of the type III and quasi-stationary continuum bursts to the moving type IV burst.

In Section 2, we describe AR 4711 above which the radio emission occurred, as well as associated activities at other wavelengths. In Section 3, we report the radio observations form the Clark Lake Radio Observatory. A brief discussion on the possibility of an associated coronal mass ejection is provided in Section 4. In Section 5, we provide a detailed discussion of the radio emission and the characteristics of the burst sources.

2. The Active Region and Hα Observations

The radio emission originated above AR 4711 which was very flare productive during its entire disk passage (Dryer *et al.*, 1986; Kundu *et al.*, 1988; Gopalswamy and Kundu, 1987, 1988a). The region was located at S 10 E49 at the time of observation and had 25 spots with a β–δ configuration. Two streamers were seen above the east limb at position angles 65° and 111° in the Mauna Loa *K*-coronameter pictures with corresponding extensions in Clark Lake quiet Sun maps.

An L shaped filament, 8° long and ~2° wide was located to the east of AR 4711. First activity in the filament was seen as early as 18:24 UT as parts of it showing upward motion and the moving part was seen faintly in emission (Martin, 1988, private communication). Increased upward mass motion in emissions was seen around 18:45 UT. By 19:01 UT, the filament became elongated and acquired an arc shape at which time, obvious mass motion was observed along the filament. The upper part of the filament started lifting at 19:19 UT. A series of Hα pictures from 19:28 to 19:52 UT in Figure 1(a) shows the evolution of the filament. A subflare started in AR 4711 at 19:36 UT, following which there was increased upward mass motion and the whole filament started disappearing. Rapid ejecta from the base of the filament were also seen at this time. The disappearance was followed by rapid downflow around 19:48 UT with small structures brightening and changing quickly. Measurements of leading edge of the filament visible in Hα resulted in the height-time diagram shown in Figure 1(b) (Martin, 1988, private communication). Note that the filament started rising steadily from 19:32 UT and acquired a constant speed of $\sim 140 \pm 40$ km s^{-1}.

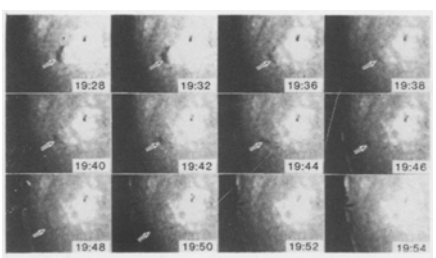

(a)

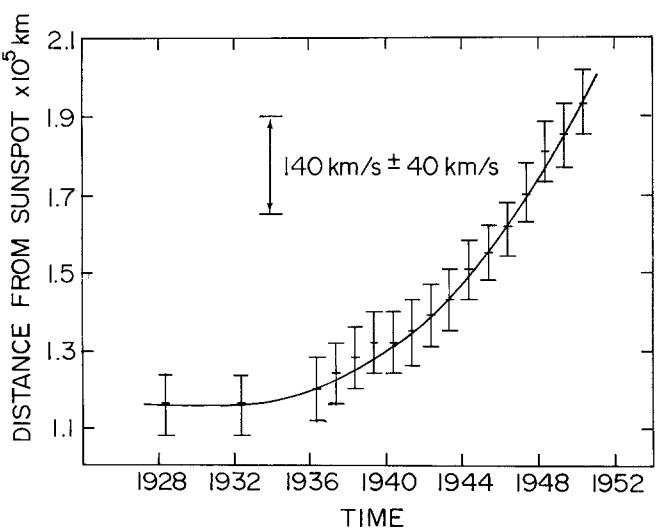

(b)

Fig. 1. (a) Evolution of the filament from 19:22 to 19:54 UT; AR 4711 is seen as the bright patch. The arrow points to the filament in question. (b) Height-time plot of the leading edge of the rising filament (courtesy: S. F. Martin).

Associated with this filament disappearance was a GOES flare of importance C 3.0, which started around 19:30 UT, maximized at 20:44 and slowly decayed for several hours. The GOES soft X-ray time profile is shown in Figure 2. There was a gradual rise and fall burst in microwaves which started at 19:35 UT, maximized at 20:57 UT and continued beyond 23:00 UT (*Solar Geophysical Data*, 1986). At the time of the flare a small plage area was rotating onto the east limb at S01 E90. This plage was associated with AR 4713 which was a bipolar region with two spots when observed at S01 E80 on February 3, 1986.

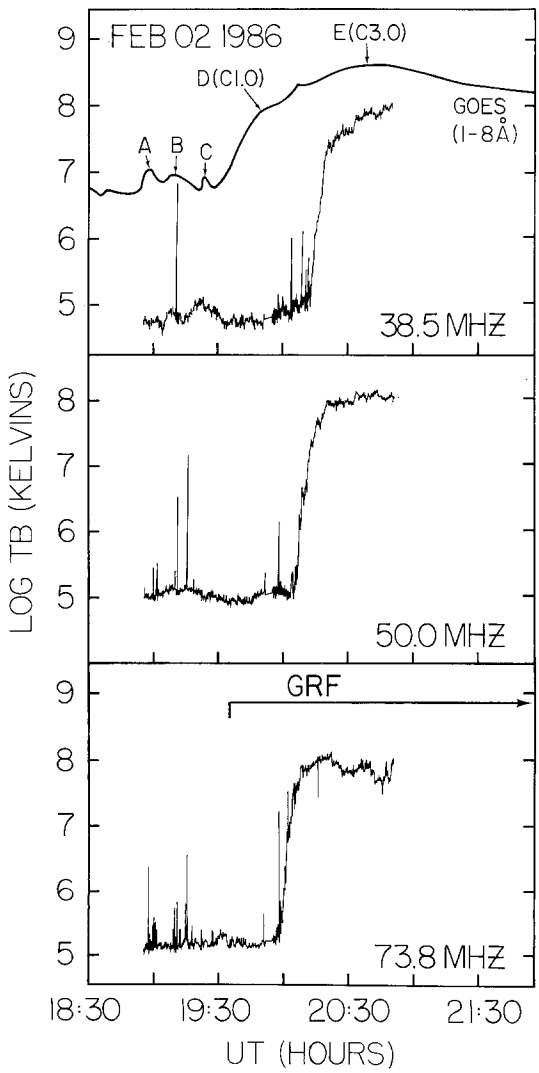

Fig. 2. Radio brightness temperature at 73.8, 50, and 38.5 MHz along with 1–8 Å GOES soft X-ray flux. The soft X-ray peaks are marked A, B, C, D, and E. The duration of the microwave gradual rise and fall (GRF) is indicated. The sharp spikes in the radio time profiles are the type III bursts; the intense rise around 20:00 UT is due to the moving type IV and quasi-stationary continuum.

3. Radio Observations

On February 2, 1986, with the Clark Lake multifrequency radioheliograph (Kundu *et al.*, 1983), we observed several weak type III bursts followed by a continuum. Shortly after the start of the continuum, a moving type IV burst was observed to separate from the continuum and move out from AR 4711. Figure 2 shows the time variation of the brightness temperature (T_b) of the radio emission. The short duration spikes are the type III bursts and the continuum starts after 20:00 UT at all three frequencies, 73.8, 50.0, and 38.5 MHz. The radio event is classified as continuum of intensity 1 from spectral observations, starting at 20:20 UT and ending at 24:00 UT (*Solar Geophysical Data*, April 1986). It is also reported as a noise storm with the spectrum extending at least to 610 MHz and probably up to 2800 MHz where it was observed as a gradual rise and fall burst (*Solar Geophysical Data*, August 1986).

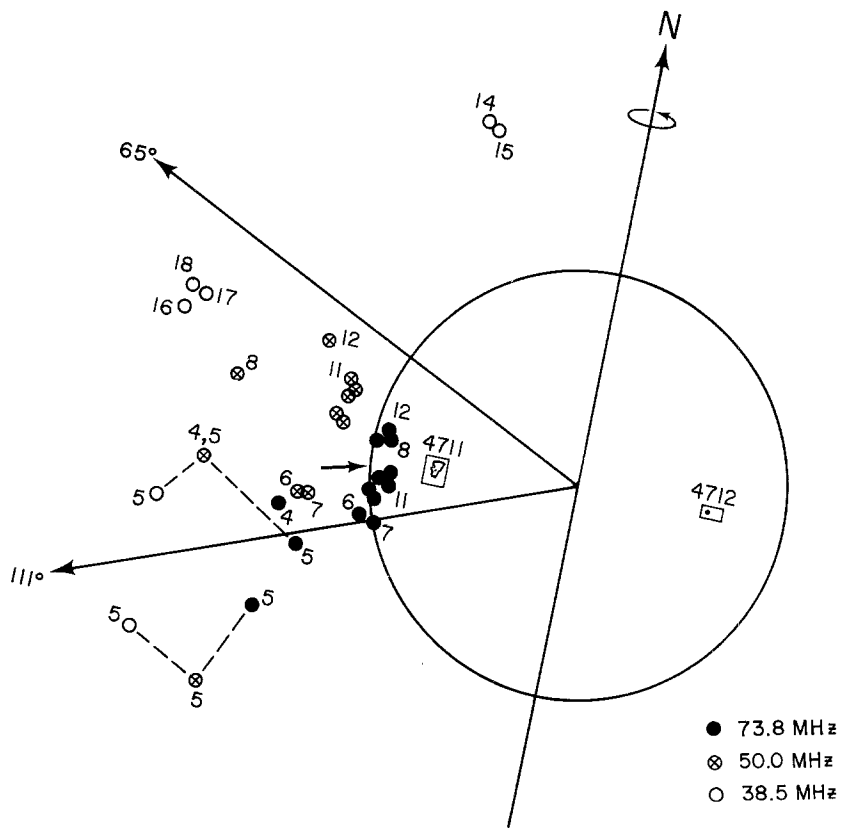

Fig. 3. Centroids of the type III bursts relative to the axes of the two streamers. The streamer axes drawn at the position angles 65° and 111° are assumed to be along the direction of maximum brightness of the streamers as observed by the Mauna Loa *K*-coronameter. The location of active regions 4711 and 4713 are indicated in the figure. Some of the centroids discussed in the text are numbered. The large circle represents the optical disk. The solar north is indicated by N.

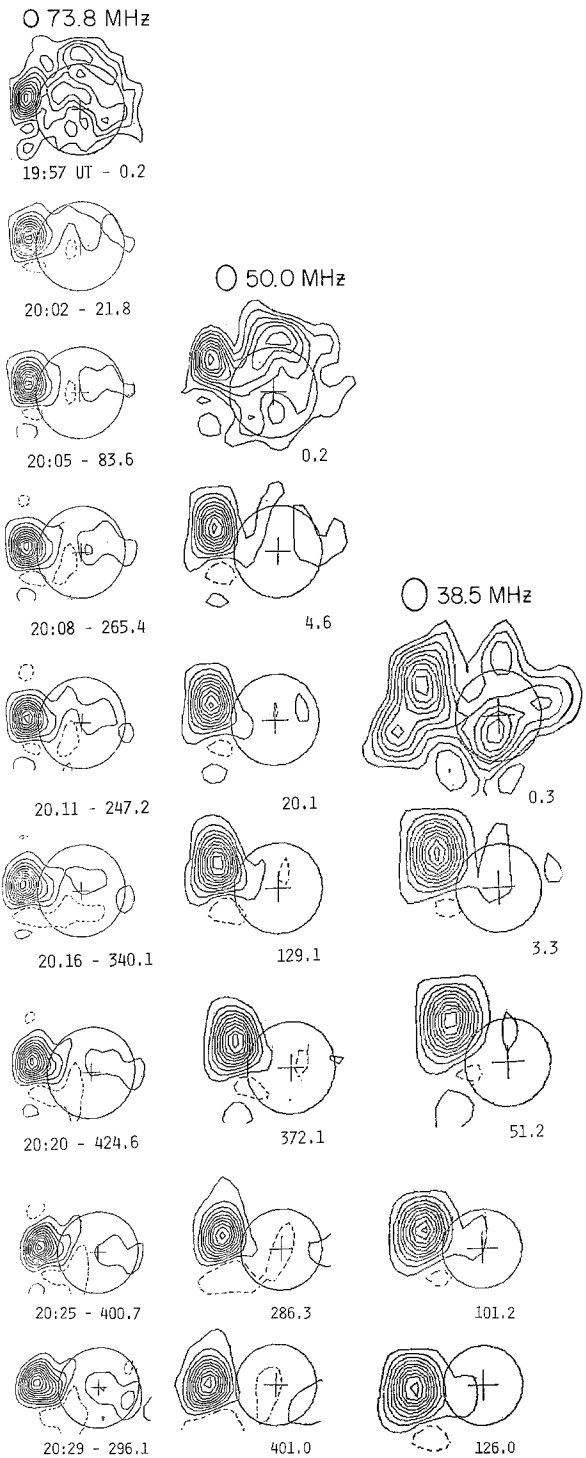
O 73.8 MHz
19:57 UT - 0.2
20:02 - 21.8
20:05 - 83.6
20:08 - 265.4
20.11 - 247.2
20.16 - 340.1
20:20 - 424.6
20:25 - 400.7
20:29 - 296.1
O 50.0 MHz
0.2
4.6
20.1
129.1
372.1
286.3
401.0
O 38.5 MHz
0.3
3.3
51.2
101.2
126.0

Fig. 4.

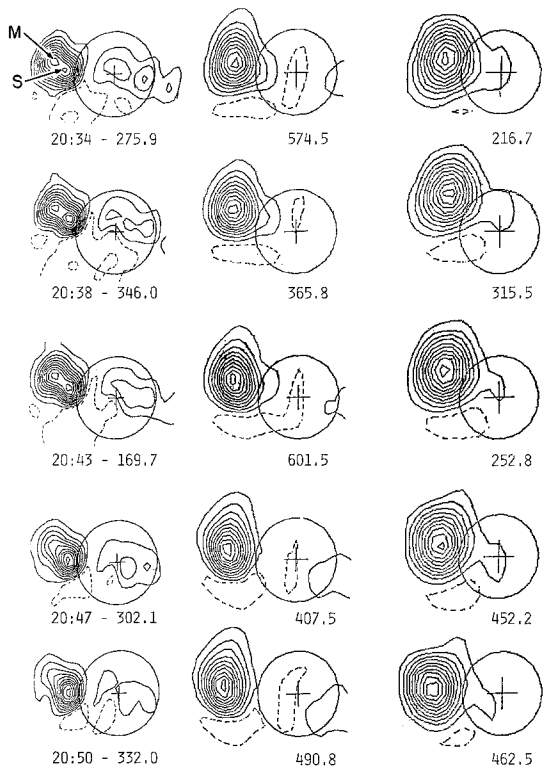

Fig. 4. Radioheliograms showing both the quasi-stationary continuum and the moving type IV bursts from ~19:57 to 20:50 UT, at 73.8, 50, and 38.5 MHz. The time of the map and the brightness temperature (in units of 10^6 K) of the stronger source are given near each map. The lowest contour is at the level of 5% of the peak brightness temperature and the contour step is 10%. The moving (M) and stationary (S) sources are marked in a 73.8 MHz map. The geocentric north is to the top and east is to the left. The circle and cross denote the optical disk and the solar center respectively. The beam sizes at each frequency are marked at the top.

Type III bursts were generally weak and only a few of them exceeded a brightness temperature of 10^7 K. A total of 19 bursts were recorded by the heliograph, but many of them were observed only at one or two frequencies. The maximum number of bursts occurred at 73.8 MHz and as the frequency decreased, the number of bursts also decreased. Whenever the bursts occurred at two frequencies, we were able to measure a forward drift of 2–12 MHz s^{-1}, typical of metric type III bursts. The bursts show clear systematic dispersion of source position with frequency. Although the bursts occurred in the same general location above AR 4711, we could identify four distinct locations. The majority of the source positions were located between the two streamer axes at position angles 65° and 111°, as shown in Figure 3. The streamer axes are assumed to be the lines of symmetry in the polar plots from Mauna Loa K-coronameter.

3.1. Continuum and moving type IV burst

The continuum started around 19:57 UT at 73.8 MHz and the onset was delayed at lower frequencies (20:04 UT at 50 MHz and 20:12 UT at 38.5 MHz). It is tempting

to classify the emission as a type II burst because of the delay at lower frequencies. But the moving and stationary sources were clearly distinguishable in the radioheliograms. Moreover, the rise time of the emission was longer than the typical type II rise time. A typical type II source remains stationary during its lifetime of several minutes, but in the present case the stationary continuum persisted for several hours (it was classified as continuum in *Solar Geophysical Data*). Therefore, we conclude that the delay is a property of the continuum source and not of a type II burst. Figure 2 shows that the onset of continuum is during the rise phase of the strongest peak of the soft X-ray burst which is an LDE. At all three frequencies, there was a sharp rise for ~ 7 min followed by a slow rise. The slow rise was longer at lower frequencies while the flux reached a maximum quasi steady level immediately after the sharp rise at 73.8 MHz. The peak brightness temperature of the continuum exceeded that of the type III bursts by two orders of magnitude (the continuum peak T_b at 73.8, 50, and 38.5 MHz were, respectively, 4.3×10^8 K, 6×10^8 K, and 4.6×10^8 K).

A closer look at the radioheliograms (Figure 4) indicates that the moving source separated from the continuum source immediately after the onset at 73.8 MHz. At this frequency, the moving burst dominated in the beginning until 20:34 UT when the two sources were distinctly seen having the same brightness temperature of $\sim 2.8 \times 10^8$ K. Thereafter, the moving source started fading while the continuum remained steady both in brightness and location. At 50 MHz, only the quasi-stationary continuum was seen until $\sim$ 20:25 UT beyond which the moving source was also detected. In this case also, it appears that the moving source was dominant. At 38.5 MHz, only the quasi-stationary source was seen and no moving source was observed until the end of observation. The observations are consistent with the onset of the continuum and the beginning of the source motion earlier at 73.8 MHz and progressively later at lower frequencies.

The radioheliograms shown in Figure 4 are not corrected for ionospheric refraction. The effect of this refraction can be seen clearly in Figure 4 by comparing the outermost contours of 38.5 MHz bursts at 20:16 and 20:29 UT. We found that the source positions at all three frequencies showed north–south and east–west quasi-periodic motions with a period of ~ 20 min. The amplitude varied inversely with the square of the frequency. This type of ionospheric refraction is caused by travelling ionospheric disturbances such as gravity waves (e.g., Stewart and McLean, 1982). The east–west (E–W) amplitude was much smaller than the north–south (N–S) amplitude and, hence, did not affect the height variation of the moving source significantly. The N–S and E–W amplitudes at 73.8, 50, and 38.5 MHz were, respectively, (0.′8, 0.′7), (2.′7, 2.′0), and (7.′5, 3.′2). The peak-to-peak amplitudes in all cases were less than the corresponding beam sizes except for the N–S case at 38.5 MHz. In this case, the peak to peak amplitude was 15.′0 as compared to the beam size of 11.′2. Since the period and amplitude of the sinusoidal variations are clearly identified, we corrected the data for these variations. The corrected positions are used for further analysis.

Figure 5 shows the evolution of the centroids of both the stationary and moving sources. The following three features are clearly seen: (i) At 50 and 38.5 MHz, the continuum sources show slow displacement parallel to the limb (southward) while the

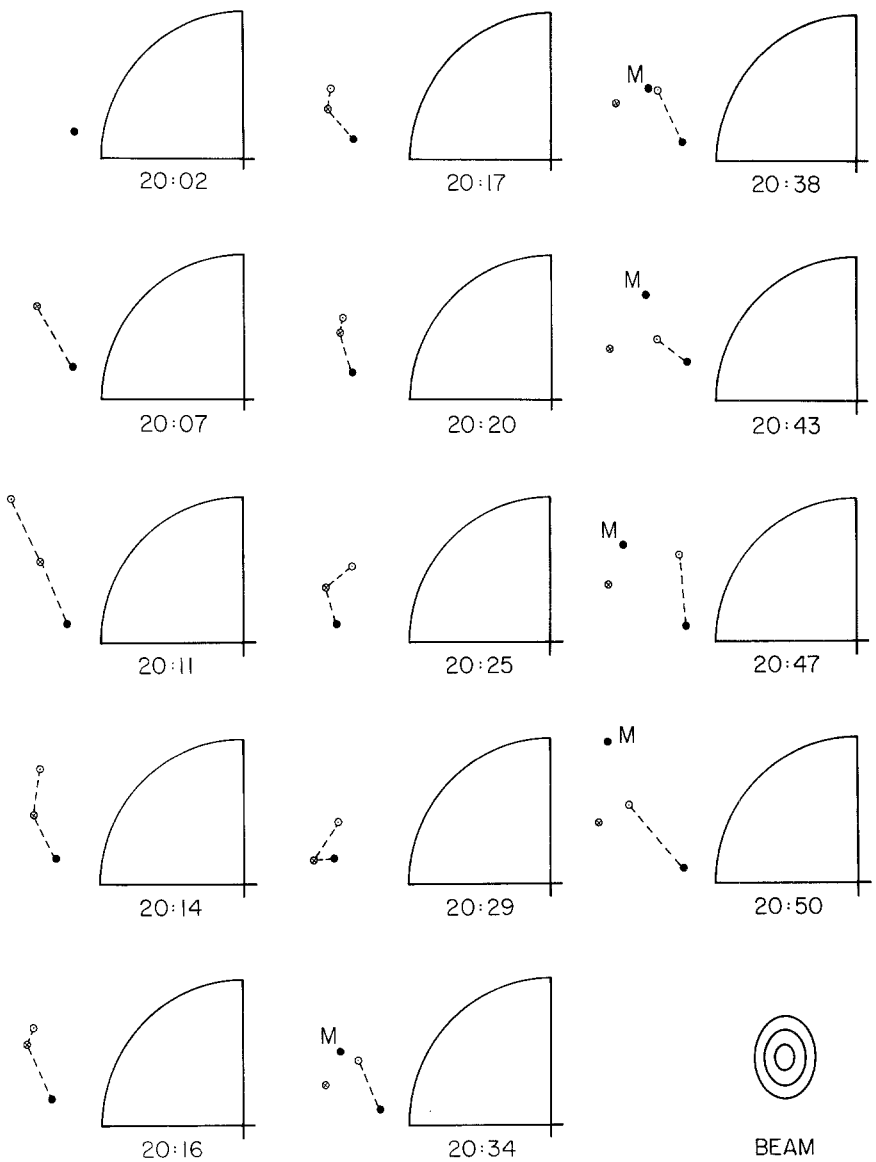

Fig. 5. Evolution of the centroids of the moving and quasi-stationary sources at three frequencies (73.8, 50.0, and 38.5 MHz) showing the dispersion of position with frequency. The north–east quadrant of the optical disk is shown. The filled circle, circle with a cross and open circle represent the 73.8, 50, and 38.5 MHz source centroids. The circles with dot denote the 73.8 MHz moving source. The inner, middle and outer ellipses indicate the 73.8, 50, and 38.5 MHz beam sizes.

73.8 MHz shows no significant displacement. The overall extent of this motion is $\sim 9'.3$ and $8'.5$ at 38.5 and 50 MHz. (ii) The 73.8 MHz moving type IV source initially moves radially outward from $\sim 20:08$ to $20:25$ UT after which the motion is in the NE direction. The 50 MHz source shows a similar tendency but the observation ended at

~ 20:50 UT and so we are not sure about the NE motion. (iii) During the radial motion, the moving type IV and the continuum sources are not resolved, although two sources are seen at 73.8 MHz (see Figure 4). When the moving type IV began its NE motion, the 73.8 MHz continuum is clearly seen at the starting location. It is thus clear that the continuum is present all the time but its centroid is masked by the moving source.

The continuum source positions showed clear dispersion with frequency as seen in Figure 5 at 20:11 UT. After this time the dispersion became complicated because of the weaker continuum source. At 20:29 UT, when the 50 MHz motion started, both 50 and 73.8 MHz moving sources are close to each other and after that the 73.8 MHz source appeared somewhat at a larger height.

The height-time variation of the continuum and moving sources are shown in Figure 6. The bottom panel shows that the 73.8 MHz continuum remains stationary throughout the observation. Before 20:34 UT, the continuum was seen but its source position could not be measured accurately as the moving source dominated. At 50 MHz (middle

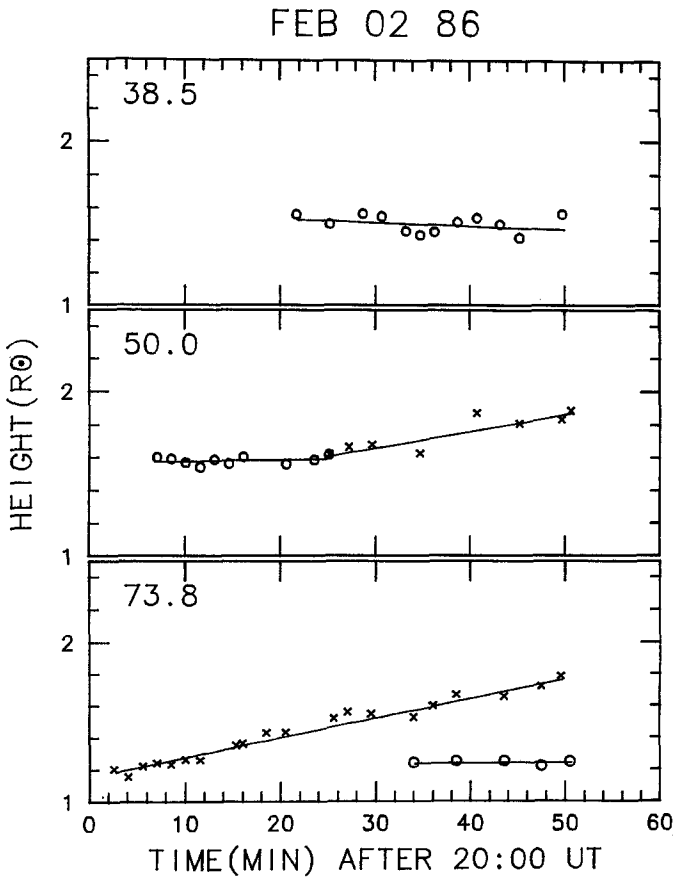

Fig. 6. Height-time plot of the moving (×) and quasi-stationary sources (○) at 73.8 MHz (bottom panel), 50 MHz (middle panel), and 38.5 MHz (top panel). The solid lines represent the least square fit to the data points.

panel), the motion starts from an initial stationary source. Again the stationary source was weaker after the onset of motion and hence the source position could not be determined. At 38.5 MHz, no moving source was seen till the end of observation. The solid curves in Figure 6 represent the best-fit, straight lines to the heights obtained after correcting for ionospheric refraction.

The speed of the moving source is 142 km s^{-1} at 73.8 MHz and 118 km s^{-1} at 50 MHz, with an average speed of $\sim$130 km s^{-1}. Obviously, this is a slowly moving type IV burst. Note that speed of the moving type IV is nearly the same as that of the leading edge of the rising filament (140 km s^{-1}). If we account for the location of the associated active region on the disk, the average speed is 172 km s^{-1}. This is much smaller than the typical speed ($\sim$400 km s^{-1}) of moving type IV bursts (Stewart, 1985). If the height-time variation of the 73.8 MHz source (which shows unambiguous motion) is extrapolated to the photosphere, the start of the event corresponds to 19:46 UT. Extrapolation of the 50 MHz plot intercepts the photosphere at $\sim$19:25 UT close to the start of the LDE.

The above starting times of 19:46 UT (73.8 MHz) and 19:25 UT (50 MHz) are not accurate because these are obtained from projected heights. Assuming that the sources moved radially above AR 4711, let us estimate the starting times. The moving sources are at projected heights of $\sim$1.21 and 1.6 $R_\odot$ at 20:11 and 20:29 UT, respectively. Since AR 4711 is on the disk (S 10 E49), the actual heights might be $\sim$1.6 and 2.12 $R_\odot$ at 73.8 and 50 MHz, respectively. Using the corrected speed of 172 km s^{-1}, the starting times become 19:31 UT (73.8 MHz) and 19:14 UT (50 MHz). If we recall the motion of the filament, we see that the upper part of the filament started lifting around 19:19 UT and attained a constant speed of $\sim$140 km s^{-1} around 19:32 UT. This is in good agreement with the starting time of the moving type IV source somewhere in the range 19:14–19:31 UT. This result is also consistent with the observations of Harrison *et al.* (1985) where the CME onsets are found to be during soft X-ray precursors before the associated LDE (see also Gopalswamy and Kundu, 1988b). We do see some soft X-ray precursors before the main LDE (marked A, B, C in Figure 1) but we are not sure whether these are related to the current event because their positions are not known.

4. Was There a CME?

From January 26, 1986, a streamer in the south–east quadrant was seen to grow stronger and was strongest when AR 4711 was just behind the limb on January 29, 1986, as seen in the Sacramento Peak coronagraph plots (*Solar Geophysical Data*, March 1986). This streamer was located radially above AR 4711. In the Mauna Loa Mark III *K*-coronameter (MLO) map, the same trend was observed, with the maximum width of the streamer extending from position angle 90 to 110°. Figure 7 shows the evolution of the streamer structure from January 29 to February 2, 1986 as seen by Mauna Loa *K*-coronameter and the Clark Lake radioheliograph. Notice that the streamer is strong at position angle $\sim$123° on January 30. Overnight (January 30–31), the streamer was depleted as seen in the Figure 7 (MLO data). Probably a coronal transient occurred

during this period (Garcia, 1988, private communication). After the depletion, a restructuring of the streamer is seen in the vicinity of the depletion on February 1; it continued on February 2, with considerable coronal brightness enhancement. Notice that the wedge shaped depletion has completely disappeared due to coronal enhancement on February 2. While the structure to the south of the depletion region remains more or less constant except probably for the rotation, the one to the north of it undergoes considerable change. The moving radio source is spatially coincident with

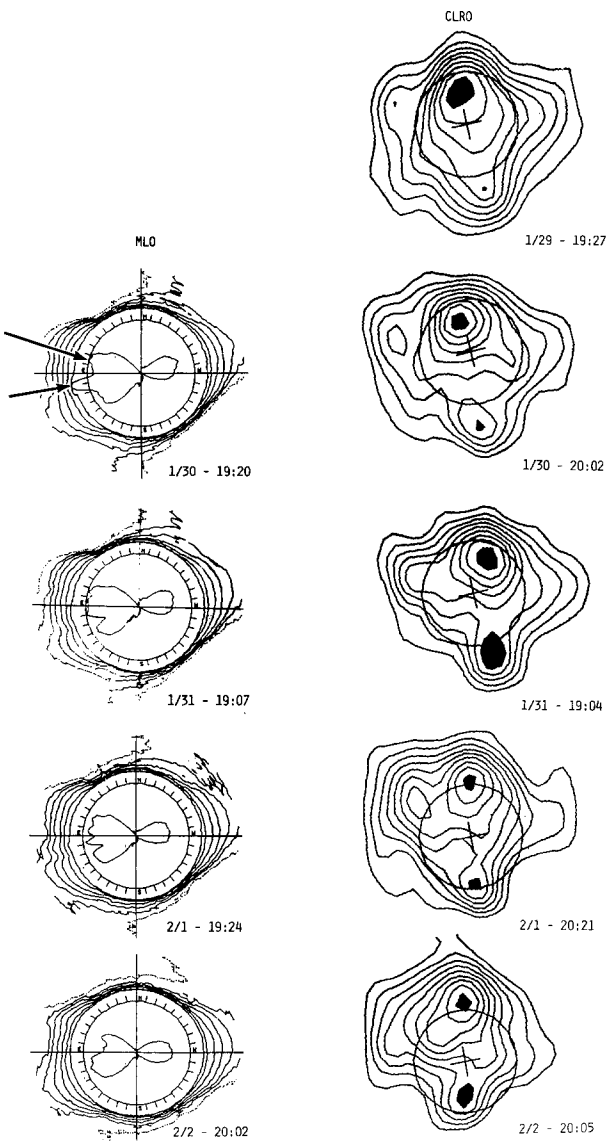

Fig. 7. Evolution of the streamer structures in the region where the radio bursts occur; Clark Lake radio maps and Mauna Loa *K*-coronameter maps. The relevant streamer structures are marked by arrows.

this northern region as seen in Figure 8 where we have superposed the centroids of 73.8 and 50 MHz moving burst sources, on the February 2, 1986 MLO map with February 1, 1986 data subtracted. As only one map per day was available from MLO for this period, we are unable to say whether the coronal enhancement seen in Figure 8 moved or not. Also, the actual extent of this enhancement is not clear because the map subtracted from the event map was obtained ~ 25 hours before the event. In any case, the presence of enhanced material at the time and height of the moving type IV burst is clear.

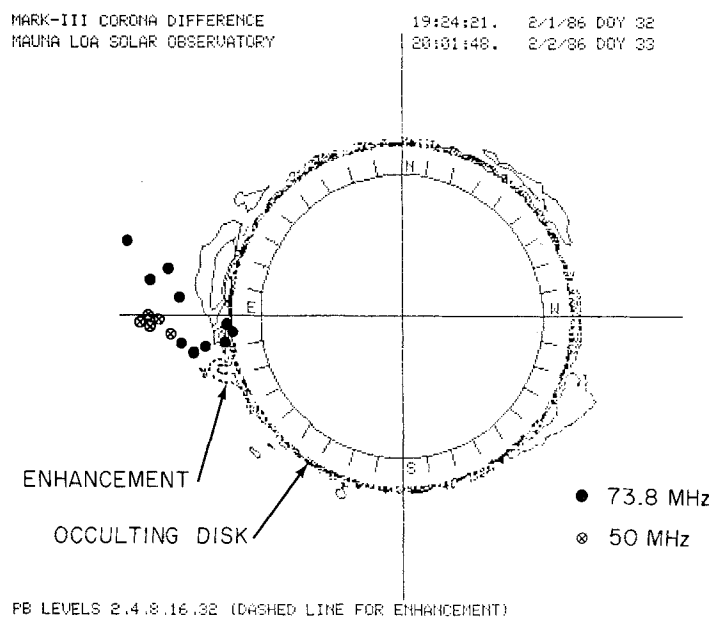

Fig. 8. Superposition of the centroids of moving type IV bursts at 73.8 MHz (filled circles) and 50 MHz (circles with crosses) on the Mauna Loa K-coronameter difference image for February 2, 1986 (February 1, 1986 image at 19:24:21 UT was subtracted from February 2, 1986 image at 20:01:48 UT). The two dashed contours to the south of the equator at position angle $\sim 110°$ represent the enhancement of polarization brightness. The contours to the north of the equator are due to streamer rotation (day-to-day difference).

5. Discussion

5.1. The type III precursors

Since type III bursts occurred before and during the continuum radio emission (storm radiation) one may wonder whether they are type I bursts. But we know that (i) the duration of type I bursts is ≤ 1 s and (ii) the source position of the type I bursts is the same as that of the associated storm continuum. Neither of these characteristics are present in this case – the duration of the bursts were several seconds and the source positions of the bursts and continuum are well separated (by $\sim 0.5\, R_\odot$). Further, the bursts are not storm type III bursts since the latter dominate at lower frequencies, contrary to the present observations (Figure 1). In fact the only type III burst at

38.5 MHz before the onset of the continuum was burst 5 (Figure 3) which occurred at a location far south of the activity center and we believe that it is due to the AR 4713 at the limb. Therefore, we conclude that the present type III bursts may be associated with the global activity of filament disappearance. The type III bursts observed here could also be viewed as the manifestation of small-scale reconnections associated with the restructuring of the corona (and the magnetic fields embedded in it) as discussed in Section 4.

The source positions of the majority of the type III bursts are scattered along almost straight lines in the N–S direction at both 73.8 and 50 MHz (Figure 3). The extent of the scatter is $\sim 6'.8$ at 73.8 MHz and $\sim 13'$ at 50 MHz. This is ~ 2.5–4.0 times larger than the peak to peak shift caused by ionospheric disturbances observed during the continuum. The ionospheric effect can be ruled out based on another fact: bursts 11 and 12 at 73.8 MHz (Figure 3) occur on the extreme ends of the scatter line, although the time difference between them is only 24 s. The ionospheric shifts occurred over a time-scale of ~ 20 min during the present observations and hence could not have caused the observed shift. It is possible that the shifts are due to injection of electron bunches along different field lines, although closely spaced, at different times. Similar electron injection was suggested during the type III bursts observed from the same active region on 3 February 1986 (Kundu *et al.*, 1988; Gopalswamy and Kundu, 1987).

Comparing the locations of 73.8 MHz type III bursts and the continuum sources we see that the type III bursts have smaller projected heights. This may be due to the fact that the open magnetic field lines along which the type III electrons propagate are closer to the direction of line of sight compared to the closed field lines along which the continuum bursts occur.

5.2. The quasi-stationary continuum

The source positions of the quasi-stationary continuum showed a typical characteristic of plasma radiation, namely the dispersion of source position with frequency. The only additional feature is the motion of the sources parallel to the limb, so that the projected height from the disk center remained nearly the same at each frequency. Similar motion of quasi-stationary continuum has also been reported earlier (McLean, 1973). Although both the moving type IV and the quasi-stationary continuum occur at the same location initially, the former does not seem to have affected the continuum source significantly. This suggests that these two bursts occur in structures located at slightly different angles from the plane of the sky, the common connection between them being possibly the supply of nonthermal electrons during the event. The initial motion parallel to the limb may be due to the coronal restructuring process that was going on even during our observations. It is also important to note that the continuum emission occurred throughout the disk passage of AR 4711 as the region was highly flare productive. The present observation is the start of the continuum which apparently was sustained by a continual supply of nonthermal particles over several days (Gopalswamy and Kundu, 1988a).

5.3. MOVING TYPE IV BURSTS

Slow coronal mass ejections and slowly moving type IV bursts are of great interest because of their association with streamer evolution (see, e.g., Illing and Hundhausen, 1986; Kundu, 1987). It is clear from the discussion in Section 4 that the corona above AR 4711 was dynamic over a period of 3 days with streamer depletion followed by coronal brightness enhancement. The moving type IV reported in this paper also seems to fall into this category with the filament eruption accompanying the ejection of material.

Among the three types of structures of moving type IV bursts (advancing front, expanding arch and isolated source) seen in radioheliograph observations (Smerd and Dulk, 1971), the present one has the appearance of an isolated source. If the nonthermal radio emission originates from this isolated plasmoid, where do the nonthermal electrons come from? There are several possibilities:

(i) During the initial lift-off of plasmoid: If the plasmoid formed during the instability of a large scale magnetic field overlying the filament then one would expect reconnection induced below the filament. As a result of this reconnection, several bunches of the accelerated particles might have got trapped into the plasmoid before it was completely detached.

(ii) Shock acceleration: As the plasmoid moves into the corona, a shock can be formed at its apex. Electrons accelerated in this shock might get trapped in the plasmoid. However, the slow moving plasmoid can produce only a slow mode shock. Particle acceleration from slow mode shocks faces serious difficulty as the self-generated fast waves upstream of the shock are not convected back into the shock which is essential for efficient acceleration (Isenberg, 1986).

Thus we may suggest that the nonthermal particles due to a reconnection process during the formation of the plasmoid are infused into the plasmoid. Although, we cannot directly relate the origin of the nonthermal particles producing type III bursts (before and during the filament eruption) to this reconnection region, the type III bursts at least indicate the presence of nonthermal particles.

Assuming that nonthermal particles are present in the plasmoid, let us now discuss the mechanism by which they emit the observed radiation. The emission mechanism of moving type IV is still controversial, the plasma and gyrosynchrotron emissions being the competing processes (Dulk, 1980; Duncan, 1980; Stewart *et al.*, 1982). Most of the observed characteristics of moving type IVs such as (i) the density of the plasmoid, (ii) dispersion of source positions with observing frequency, (iii) polarization, and (iv) brightness temperature could be explained in terms of either mechanism, with some exceptions.

One of the important aspects which makes the gyrosynchrotron mechanism successful at least in some moving type IV bursts is an explanation of why the degree of polarization increases during its decay phase. As the source moves out, the self-absorption decreases and the X-mode becomes dominant, resulting in high degrees of polarization. However, limb sources should not have such high polarization as the viewing angle becomes

$> 60°$. This is contrary to several observations which show high polarization ($\sim 80\%$) for limb sources (Robinson, 1978). On the other hand, the plasma emission mechanism fails to provide any convincing explanation for the increase in polarization during the decay phase.

The peak brightness temperature as high as 10^{10} K, sometimes observed in moving type IV sources, cannot be explained by gyrosynchrotron models, as the electron energy needed becomes unrealistically high and the polarization almost vanishes. Plasma emission from 10–100 keV can explain this high brightness temperature, provided the nonthermal electron distribution is highly anisotopric. However, for a plasmoid configuration, there is no loss cone and the distribution is essentially isotropic. With an isotropic gap distribution, the brightness temperature is limited to $< 3 \times 10^9$ K (Goldman and Smith, 1986).

The above discussion shows that both plasma and gyroresonance emissions are capable of explaining moving type IV emission with brightness temperature $\leq 10^9$ K. In the present case we have a peak brightness temperature of only 6×10^8 K. As we have neither polarization nor density information for the plasmoid, it is difficult to identify the emission mechanism decisively. We provide some indirect arguments which support gyrosynchrotron emission.

In addition to the plasmoid being dense enough to support plasma emission, it should contain nonthermal particles with a favourable unstable distribution that can feed energy to the plasma waves. Isotropic power law distribution may not produce observable radiation at metric wavelengths (Melrose, 1980). The only possibility is an isotropic gap distribution. Melrose (1975) explored the plasma emission from isotropic gap distribution to explain radio bursts of type I, II, stationary IV and V, excluding moving type IVs. Isotropic gap distribution can form due to collisional separation of fast and slow particles or through the resonant scattering of fast particles by whistler waves. Collisional effects do not form a sharply defined gap. Formation of the gap through resonant scattering needs an anisotropic nonthermal electron distribution to generate whistlers which in turn scatter the fast particles. While this may be possible in a magnetic loop configuration, it may not apply to an isolated plasmoid (Goldman and Smith, 1986).

It is interesting to note that the moving type IV was not observed at 38.5 MHz until the end of the observation. This means, the brightness temperature of the moving source might have been less than $\sim 2 \times 10^7$ K (5% of the peak brightness temperature of the quasi-continuum source). On the other hand, the theory of Melrose (1975, his Equation (53)) predicts that the brightness temperature of the second harmonic radiation is inversely proportional to the fourth power of plasma frequency. This implies that the brightness temperatures at 50 and 38.5 MHz must be larger than that at 73.8 MHz by factors 5 and 14, respectively, contrary to the present observation. Hence, we conclude that the observed moving type IV may not be due to a plasma emission process.

The spectrum of the moving type IV burst could not be determined accurately because the moving source was not observed at 38.5 MHz before the end of the observation. However, using 50 and 73.8 MHz data, we found that the 50 MHz source was brighter.

One way of interpreting the lack of moving type IV emission at 38.5 MHz is by Razin suppression. If the emission is due to gyrosynchrotron process, we expect the 73.8 MHz emission to be optically thin and the peak emission to be somewhere between 50 and 73.8 MHz. The brightness temperature T_b of the source at frequency f with a line-of-sight dimension L_s can be related to the optical depth τ_f and emissivity η_f by (see, e.g., Dulk, 1985)

$$T_b = T_{\text{eff}}\,\tau_f = \frac{c^2}{k_B f^2}\,\eta_f L_s\,, \tag{1}$$

where $k_B T_{\text{eff}}$ is the effective temperature (in energy units) of the emitting electrons given by the average electron energy E_0; k_B is the Boltzman constant and c is the velocity of light.

If the nonthermal particles trapped in the magnetic field B have a density n_s and a power-law spectrum with index δ, the emissivity is given by the approximate formula

$$\eta_f = 3.3 \times 10^{-24} \times 10^{-0.52\delta} (\sin\theta)^{-0.43+0.65\delta} \left(\frac{f}{f_B}\right)^{1.22-0.9\delta} B n_s\,, \tag{2}$$

where θ is the angle between the line-of-sight and the magnetic field, and $f_B = 2.8 \times 10^6 B$ Hz is the electron cyclotron frequency. Based on the location of the active region, we assume $\theta \sim 60°$. We also assume a typical spectral index δ of ~ 4. The observed source diameter of $\sim 0.4\,R_\odot$ is taken to be the line-of-sight depth L_s of the source region. Using Equations (1) and (2) and the observed peak brightness temperature of 4.25×10^8 K at $f = 73.8$ MHz, we obtain, numerically,

$$B^{3.8} n_s = 1.53 \times 10^6\,, \tag{3}$$

which implies that the nonthermal particles of density $\sim 10^6$ cm^{-3} have to be trapped in a magnetic field of ~ 1.1 G to explain the observed radiation. The cyclotron harmonic numbers at this magnetic field strength for 73.8, 50, and 38.5 MHz frequencies are 23, 16, and 12, respectively. Increasing the magnetic field by a factor of 2, the density of nonthermal particles needed decreases by an order of magnitude and the harmonic numbers become 12, 8, and 6 at 73.8, 50, and 38.5 MHz, respectively. The magnetic field strength of 1–2 G seems to be a reasonable estimate (Gopalswamy and Kundu, 1988b).

In order to verify our results, let us estimate the peak frequency of emission, which we expect to be somewhere between 50 and 73.8 MHz. The peak frequency f_{pk} is given by (Dulk, 1985)

$$f_{pk} = 2.72 \times 10^3 \times 10^{0.27\delta} (\sin\theta)^{0.41+0.03\delta} (n_s L_s)^{0.32-0.03\delta} B^{0.68+0.03\delta}\,. \tag{4}$$

Substituting B = 1–2 G from the above estimate, we get $f_{pk} \sim 65$–70 MHz which is in the range expected. At 50 MHz the emission must be optically thick ($\tau_f \geq 1$) and so the effective temperature of the nonthermal electrons must be the observed brightness temperature ($T_b = 6.02 \times 10^8$ K). Therefore, the average electron energy is $E_0 = k_B T_b \sim 52$ keV.

For a magnetic field of ~ 2 G, the brightness temperature (T_b) of the 50 MHz radiation predicted by optically thick gyrosynchrotron emission (7.9×10^8 K) is very close to that observed (6.02×10^8 K). This implies that the medium suppression is minimal at this frequency. The predicted T_b at 38.5 MHz is 6.3×10^8 K. If the lack of 38.5 MHz emission is due to Razin effect, then its emission might have been suppressed at least by a factor of 3.8×10^{-2} so that it is masked by the quasi-continuum source. According to the theory of Razin suppression (e.g., Kaplan and Tsytovich, 1973), the emission is suppressed by a factor

$$\frac{T_b^m}{T_b^v} = \left(1 + \frac{f_p^2}{f^2}\,\gamma^2\right)^{3/4} \exp\left\{-\frac{f}{\frac{3}{2} f_B\,\gamma^2 \sin\theta}\left[\left(1 + \frac{f_p^2}{f^2}\,\gamma^2\right)^{3/2} - 1\right]\right\}, \quad (5)$$

where the superscripts m and v are used to denote T_b with medium suppression and vacuum, respectively, and f_p is the electron plasma frequency in the plasmoid. For $B \sim 2$ G and $f = 38.5$ MHz, $\gamma = 1.1$ (the relativistic factor corresponding to $E_0 \sim 50$ keV), and assuming $T_b^m = 2.4 \times 10^7$ K (which is 5% the peak of the quasi-continuum source), we get $f_p \sim 23$ MHz. This corresponds to a density of $\sim 6.6 \times 10^6$ cm^{-3} for the thermal electrons in the plasmoid. The required nonthermal electron density ($\sim 10^5$ cm^{-3}) is only $\sim 1.5\%$ of the plasmoid density.

Although the actual source may be inhomogeneous, especially when the 50 and 73.8 MHz are not co-spatial, the above estimates provide rough values of the source parameters which are reasonable. We could make approximate corrections for ionospheric effects; but coronal scattering and refraction could still be present which may be the reason for the different 50 and 73.8 MHz locations. The present estimates indicate that low-energy electrons (~ 50 keV) spiralling in relatively weak magnetic fields (~ 1–2 G) are capable of producing the observed emission. It is important to note that the only other information about nonthermal particles comes from the type III bursts. While the energy of the electrons generating type III bursts is in the range 10–50 keV, the density relative to the ambient medium is low. However, the type III bursts occur along open field lines and the electrons generating them propagate away. Since the plasmoid traps the electrons one might expect accumulation of nonthermal particles and, therefore, an increase in number density. The presence of type III electrons during the onset phase of moving type IV bursts, therefore, suggests that the trapped electrons also have energies similar to the type III electrons. The source of trapped particles may be the same as that of the type III electrons or an acceleration process during the filament disappearance.

6. Summary and Conclusions

(i) The moving type IV burst is strong evidence for material ejection into the corona in the present event. The speed of the moving type IV burst is the same as that of the leading edge of the associated erupting prominence. It is possible that the plasmoid is formed out of the heated material at the top of the rising filament. Although streamer

evolution and coronal restructuring accompanied by coronal brightness enhancement were observed over a period of 3 days before the event by the Mauna Loa *K*-coronameter, motion of white light material could not be established due to lack of data. However, the observed coronal brightness enhancement was in the vicinity of the moving type IV burst both temporally and spatially. One such slowly moving type IV burst was reported by Kundu (1987) which was associated with a coronal streamer disruption event. A coronal streamer disruption event occurs after a few days of coronal streamer changes as observed in the present case.

(ii) Comparison of the relative locations of the type III bursts, the moving type IV bursts and the quasi stationary continuum suggests that different magnetic structures above the same active region received a supply of nonthermal electrons generated low in the corona, which produced appropriate radio emissions determined by the local conditions in the source regions.

(iii) The moving type IV burst could be interpreted in terms of Razin suppressed gyrosynchrotron emission from nonthermal electrons of average energy ~ 50 keV and number density $\sim 10^5$–10^6 cm^{-3} trapped in a plasmoid. From the observed characteristics of the radio emission, the magnetic field in the plasmoid is estimated to be ~ 1–2 G. The absence of moving type IV emission at 38.5 MHz can be interpreted as due to Razin suppression which provides a lower limit of $\sim 6.6 \times 10^6$ cm^{-3} to the density of the plasmoid.

Acknowledgements

We thank Drs S. M. White and E. J. Schmahl for a critical reading of the manuscript and helpful comments. We thank Ms S. F. Martin for the filament data from Big Bear Solar Observatory. The Mark III *K*-coronameter data are from Mauna Loa Solar Observatory (High Altitude Observatory) operated by the National Center for Atmospheric Research. The data were kindly provided to us by Dr C. J. Garcia. We also thank Dr C. J. Garcia for a disussion on the streamer evolution and coronal enhancement. The authors have benefited from discussions with many participants of the second SEIIM Workshop (1988, Colorado Springs, Colorado) where part of the results was presented. Partial computational support was provided by the University of Maryland Computer Science Center. We thank the anonymous referee for suggestions that significantly improved the presentation of the paper. This research was supported by the NSF grant ATM 88–16008 and by grants from the Astronomy Program and the College of Computer, Mathematical and Physical Sciences of the University of Maryland.

References

Dryer, M., Smith, Z. K., Detman, T. R., and Yeh, T.: 1986, *Air Force Geophysical Laboratory Report* (in press).
Dulk, G. A.: 1980, in M. R. Kundu and T. E. Gergely (eds.), 'Radio Physics of the Sun', *IAU Symp.* **86**, 419.
Dulk, G. A.: 1985, *Ann. Rev. Astron. Astrophys.* **23**, 169.
Duncan, R. A.: 1980, *Proc. Astron. Soc. Australia* **4**, 67.
Garcia, C. J.: 1988, private communication.

Goldman, M. V. and Smith, D. F.: 1986, in P. A. Sturrock, T. E. Holzer, D. M. Mihalas, and R. K. Ulrich (eds.), *Physics of the Sun*, Vol. II, D. Reidel Publ. Co., Dordrecht, Holland, p. 325.
Gopalswamy, N. and Kundu, M. R.: 1987, *Solar Phys.* **111**, 347.
Gopalswamy, N. and Kundu, M. R.: 1988a, *Proc. of the STIP Symposium on Physical Interpretation of Solar/Interplanetary and Cometary Intervals*, Huntsville, 1987 (in press).
Gopalswamy, N. and Kundu, M. R.: 1988b, *Solar Phys.* **114**, 347.
Harrison, R. A., Wagget, P. W., Bentley, R. D., Phillips, K. J. H., Bruner, M., Dryer, M., and Simnett, G. M.: 1985, *Solar Phys.* **97**, 387.
Hundhausen, A. J., Holzer, T. E., and Low, B. C.: 1987, *J. Geophys. Res.* **92**, 11173.
Illing, R. M. E. and Hundhausen, A. J.: 1986, *J. Geophys. Res.* **91**, 10951.
Isenberg, P. A.: 1986, *J. Geophys. Res.* **91**, 1699.
Kaplan, S. A. and Tsytovich, V. N.: 1973, *Plasma Astrophysics*, Pergamon Press, New York.
Kuin, N. P. and Martens, P. C. H.: 1986, in A. I. Poland (ed.), *Coronal and Prominence Plasmas*, NASA Conference Publication 2442, p. 241.
Kundu, M. R.: 1987, *Solar Phys.* **111**, 53.
Kundu, M. R., Erickson, W. C., Gergely, T. E., Mahoney, ML. J., and Turner, P. J.: 1983, *Solar Phys.* **83**, 385.
Kundu, M. R., Gopalswamy, N. Saba, J. L. R., Schmelz, J. T., and Strong, K. T.: 1988, *Solar Phys.* **114**, 273.
Martin, S. F.: 1973, *Solar Phys.* **31**, 3.
Martin, S. F.: 1988, private communication.
Martin, S. F. and Ramsey, H. E.: 1972, in P. McIntosh and M. Dryer (eds.), *Solar Activity, Observations and Predictions*, MIT, Cambridge, p. 371.
McLean, D. J.: 1973, *Proc. Astron. Soc. Australia* **2**, 222.
Melrose, D. B.: 1975, *Solar Phys.* **43**, 211.
Melrose, D. B.: 1980, *Plasma Astrophysics*, Gordon and Breach, New York, Vol. II, p. 190.
Moore, R. L., Horwitz, J. L., and Green, J. L.: 1984, *Planetary Space Sci.* **32**, 1439.
Munro, R. H., Gosling, J. T., Hildner, E., MacQueen, R. M., Poland, A. E., and Ross, C. L.: 1979, *Solar Phys.* **61**, 201.
Robinson, R. D.: 1978, *Solar Phys.* **60**, 383.
Smerd, S. F. and Dulk, G. A.: 1971, in R. Howard (ed.), 'Solar Magnetic Fields', *IAU Symp.* **43**, 616.
Smith, S. F. and Ramsey, H. E.: 1964, *Z. Astrophys.* **60**, 1.
Stewart, R. T.: 1985, in D. J. McLean and N. R. Labrum (eds.), *Solar Radio Physics*, Cambridge Univ. Press, Cambridge, 14, p. 361.
Stewart, R. T. and McLean, D. J.: 1982, *Proc. Astron. Soc. Australia* **4**, 396.
Stewart, R. T., McCabe, M. K., Koomen, M. J., Hansen, R. T., and Dulk, G. A.: 1974, *Solar Phys.* **36**, 203.
Stewart, R. T., Dulk, G. A., Sheridan, K. V., House, L. L., Wagner, W. J., Sawyer, C. J., and Illing, R.: 1982, *Astron. Astrophys.* **116**, 217.
Tandberg-Hanssen, E., Martin, S. F., and Hansen, R. T.: 1980, *Solar Phys.* **65**, 357.
Webb, D. F. and Jackson, B. V.: 1981, *Solar Phys.* **73**, 341.